Electronic Supplementary Information (ESI) for:

Continuous droplet electroporation system for high throughput processing

Byeong Sun Yoo,[a] Do Jin Im,[*,b] Myung Mo Ahn,[a] Sung Jin Park,[b] Yeong Hun Kim,[b] Tae Woong Um[a] and In Seok Kang[a]

[a]Department of Chemical Engineering, Pohang University of Science and Technology, 77 Cheongam-Ro, Nam-Gu, Pohang, Gyeongbuk, South Korea 37673

[b]Department of Chemical Engineering, Pukyong National University, 365 Sinseon-Ro, Nam-Gu, Busan, South Korea 48547

CORRESPONDING AUTHOR:

Email: dj-im@pknu.ac.kr

Contents:

1. Comparison of flow characteristics depending on the flow direction of cell suspension

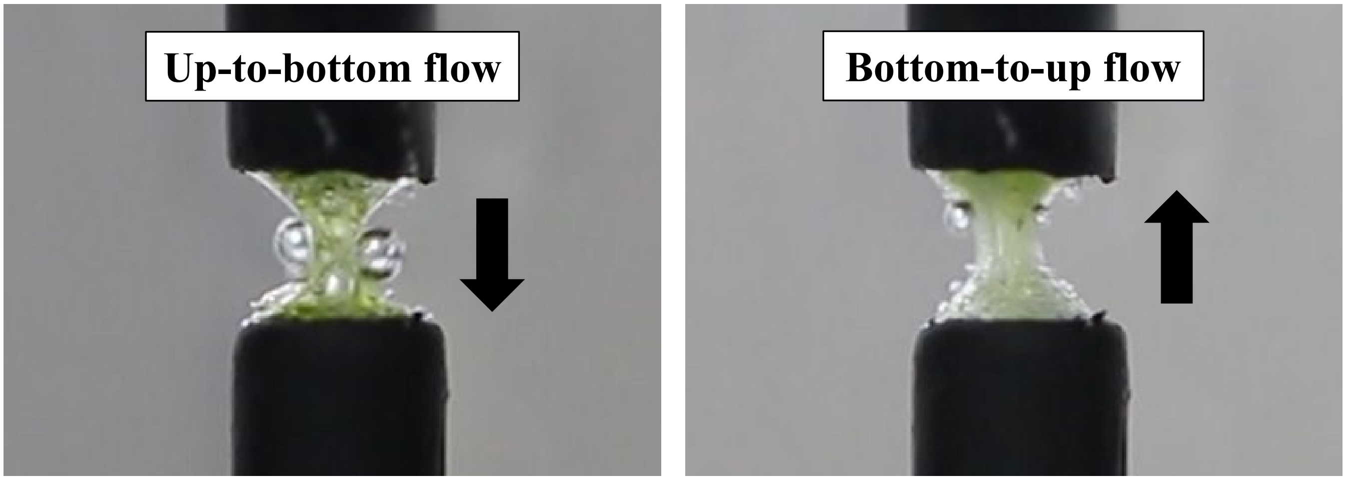

Fig. S1. Bottom-to-up vs. up-to-bottom flow direction for the continuous droplet EP system.

Because of gravity, the choice of flow direction in the continuous droplet EP system can largely influence the flow characteristics as shown in Fig. S1. We chose the bottom-to-up flow for efficient removal of gas bubbles. When the up-to-bottom flow was used, the gas bubble removal was not efficient because the direction of bubble movement and the cell suspension flow were opposite, which cause gas bubble entrapment near liquid bridge as shown at the left of Fig. S1. On the other hand, when the bottom-to-up flow was used, the gas bubbles were efficiently removed because the direction of bubble movement and the cell suspension flow were in line, which helped the removal of gas bubbles.

2. Numerical simulation details

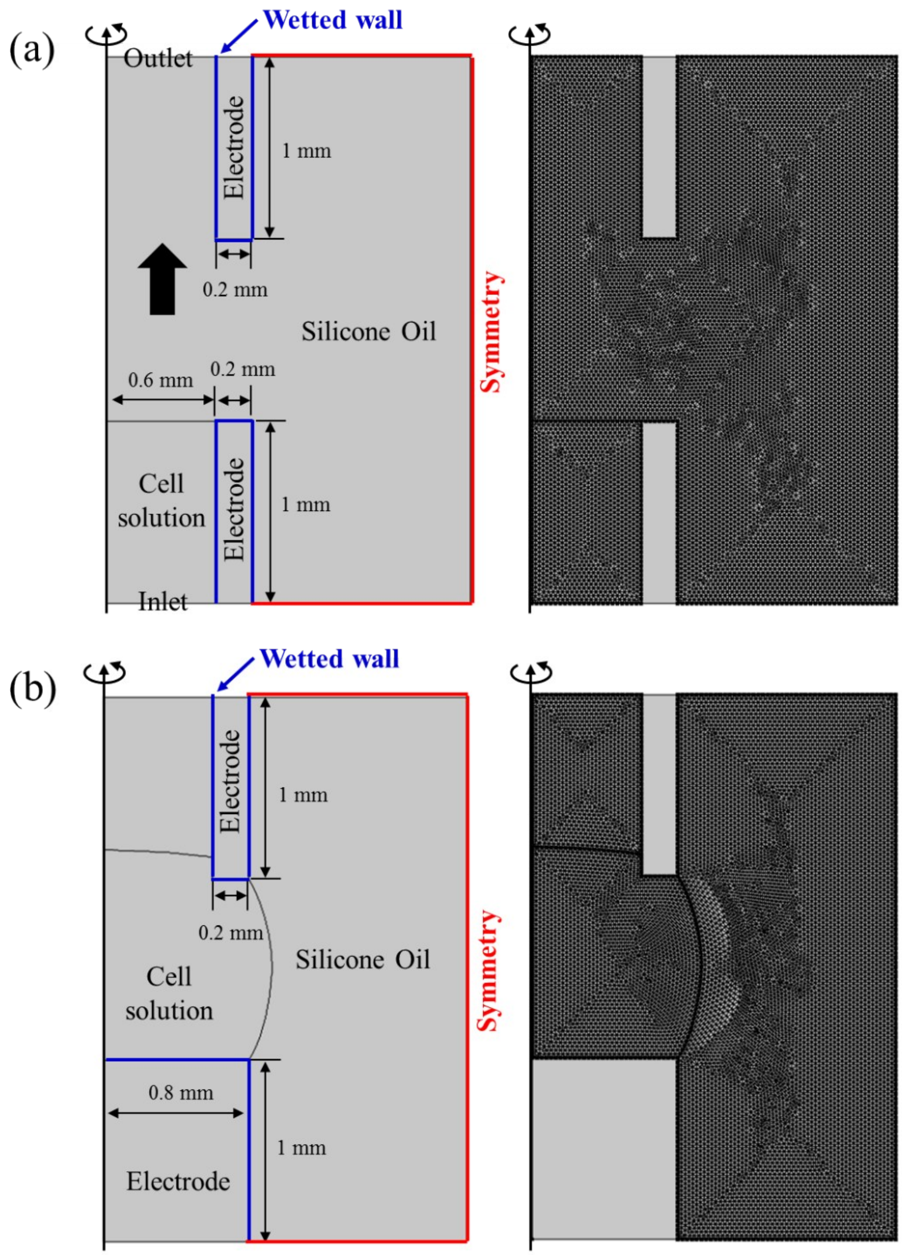

Fig. S2. Geometry and mesh of (a) the continuous droplet EP system and (b) the single droplet EP system.

All numerical simulations were conducted in the manner of two dimension axial-symmetry using the Phase field method and electrostatics model in COMSOL Multiphysics. The fluid flow was analyzed by solving the Navier-Stokes equation and Continuity equation:

$$\rho(\varphi)\left(\frac{\partial u}{\partial t} + u \cdot \nabla u\right) = \nabla \cdot \left[-p + \mu(\varphi)\left(\nabla u + (\nabla u)^T\right)\right] + F_{surf} + F_{ext} \tag{s1}$$

$$\nabla \cdot u = 0 \tag{s2}$$

φ is the phase field order parameter that takes the value φ = -1 in one phase and φ = 1 in the other phase, ρ and μ are the density and viscosity of the two phases, where the material properties are interpolated as

$$\rho = \left(\frac{1-\varphi}{2}\right)\rho_{oil} + \left(\frac{1+\varphi}{2}\right)\rho_{cell} \tag{s3}$$

$$\mu = \left(\frac{1-\varphi}{2}\right)\mu_{oil} + \left(\frac{1+\varphi}{2}\right)\mu_{cell} \tag{s4}$$

$\mathbf{F}_{surf}$ is the surface tension force, and $\mathbf{F}_{exrt}$ is the external body force. Wetted wall condition of electrodes were 9π/20 radian.

Phase Field interface was governed by a Chan-Hilliard equation:

$$\frac{\partial\varphi}{\partial t} + u\cdot\nabla\varphi = \nabla\cdot\frac{\gamma\lambda}{\varepsilon^2}\nabla\psi \tag{s5}$$

$$\psi = -\nabla\cdot\varepsilon^2\nabla\varphi + (\varphi^2-1)\varphi \tag{s6}$$

where **u** is the velocity field, γ is the mobility, λ is the mixing energy density and ε is the interface thickness parameter. The ψ is referred to as the phase field help variable.

The electric field distribution of the system was obtained by the following Laplace equation:

$$\nabla^2\phi = 0 \tag{s7}$$

where ϕ is the electric potential. In the simulations, the dielectric constants of the silicone oil and the cell suspension are 2.78 and 78, respectively. The bottom electrodes were set as ground and the upper electrode were set various electric potential from 64 V to 192 V for the boundary conditions. ($\partial\phi/\partial n = 0$ at remaining domain boundaries). The electrical conductivity of cell suspension was 213 mS/m.

3. Comparison between the continuous droplet EP system and the single droplet EP system

To visualize the electric field strength according to the position of cells, particles were distributed in the cell suspension as shown in Fig S3. The average value of electric field strength exerted on particles was calculated in Table S1. In the single droplet EP system, most particles were exposed to average electric field strength (around 1 kV/cm) and only very few particles around the upper electrode were exposed to high electric field (around 2 kV/cm) as shown in Fig. S3a. In the continuous droplet EP system, fluid flow of cell suspension through the inlet-outlet system was computed before investigating electric field strength because the electric field distribution changes continuously according to the fluid flow. Two representative electric field distribution of the continuous droplet EP system was visualized as shown in Figs. S3b and S3c. Fig. S3b shows the moment of droplet contact to an upper electrode which is similar to the single droplet EP system and Fig. S3c shows the moment right before the liquid bridge breakup occurs, when particles are exposed to high electric field (around 2 kV/cm) near liquid bridge.

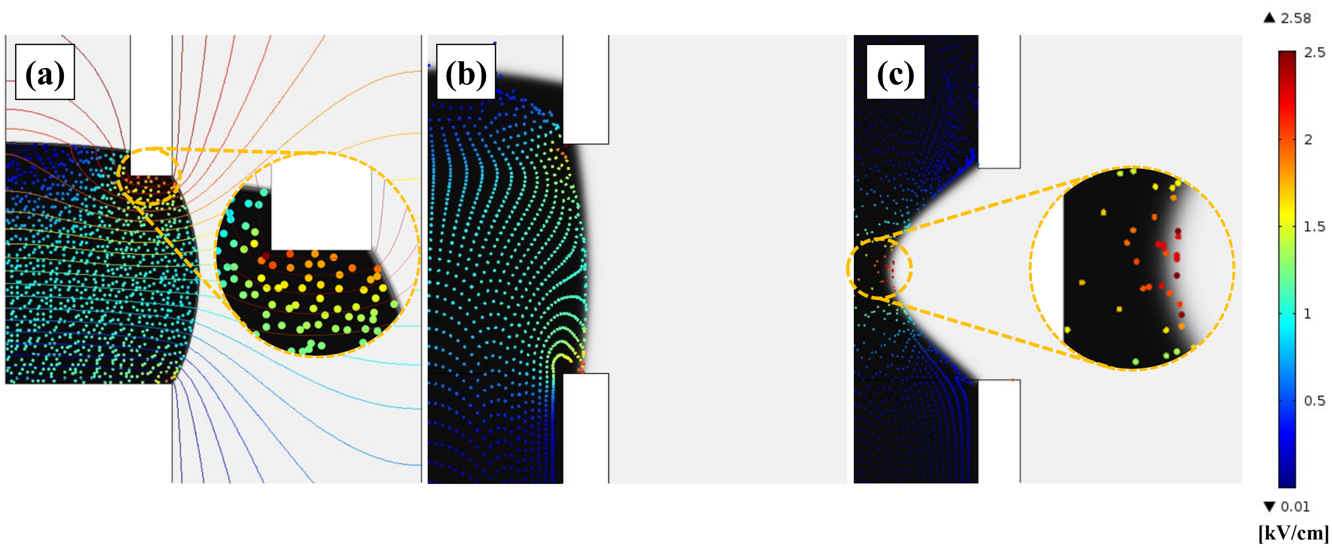

Fig. S3. The electric filed distribution in the single droplet EP system and the continuous droplet EP system. Electric field strength affecting to each cell was visualized at the applied voltage of 128 V. (a) Single droplet EP, (b) Continuous droplet EP at the similar situation to the single droplet EP, (c) Continuous droplet EP at the moment of liquid bridge formation.

Table S1. Average electric field strength of the single droplet EP system and the continuous droplet EP system.

Applied voltage	Single Droplet EP [kV/cm]	Cont. Droplet EP [kV/cm]	Cont. Droplet EP (Yellow zone) [kV/cm]
64 V	0.53	0.49	1.02
128 V	1.05	0.99	1.98
192 V	1.58	1.48	2.99